(i) From the x axis to the optic axis, $\mathbf{e}^o$ and $\mathbf{e}^e$ are given by (1.7.3.11) and (1.7.3.12) with $\varphi = 0$. The walk-off is relative to the extraordinary wave and is calculated from (1.7.3.13) with $n_o = n_x$ and $n_e = n_z$.

(ii) From the optic axis to the z axis, the vibration plane of the ordinary and extraordinary waves corresponds respectively to a rotation of $\pi/2$ of the vibration plane of the extraordinary and ordinary waves for a propagation in the areas of the principal planes of opposite sign; the extraordinary electric field vector is given by (1.7.3.12) with $\varphi = 0$, $-\rho^-(\varphi, \omega)$ for the positive class and $+\rho^+(\varphi, \omega)$ for the negative class, and the ordinary electric field vector is out of phase by π in relation to (1.7.3.11), that is

$$e_x^o = 0 \quad e_y^o = -1 \quad e_z^o = 0. \tag{1.7.3.17}$$

The extraordinary walk-off angle is given by (1.7.3.13) with $n_o = n_x$ and $n_e = n_z$.

The $\pi/2$ rotation on either side of the optic axes is well observed during internal conical refraction (Fève *et al.*, 1994).

Note that for a biaxial crystal, the walk-off angles are all nil only for a propagation along the principal axes.

1.7.3.1.4.2. *Propagation out of the principal planes*

It is impossible to define ordinary and extraordinary waves out of the principal planes of a biaxial crystal: according to (1.7.3.6) and (1.7.3.9), $\mathbf{e}^+$ and $\mathbf{e}^-$ have a nonzero projection on the z axis. According to these relations, it appears that $\mathbf{e}^+$ and $\mathbf{e}^-$ are not perpendicular, so relation (1.7.3.10) is never verified. The walk-off angles ρ^+ and ρ^- are nonzero, different, and can be calculated from the electric field vectors:

$$\rho^{\pm}(\theta, \varphi, \omega) = \varepsilon \arccos[\mathbf{e}^{\pm}(\theta, \varphi, \omega) \cdot \mathbf{u}(\theta, \varphi, \omega)] - \varepsilon\pi/2. \tag{1.7.3.18}$$

$\varepsilon = +1$ or -1 for a positive or a negative optic sign, respectively.

1.7.3.2. *Equations of propagation of three-wave and four-wave interactions*

1.7.3.2.1. *Coupled electric fields amplitudes equations*

The nonlinear crystals considered here are homogeneous, lossless, non-conducting, without optical activity, non-magnetic and are optically anisotropic. The nonlinear regime allows interactions between γ waves with different circular frequencies $\omega_i, i = 1, \ldots, \gamma$. The Fourier component of the polarization vector at ω_i is $\mathbf{P}(\omega_i) = \varepsilon_0 \chi^{(1)}(\omega_i)\mathbf{E}(\omega_i) + \mathbf{P}^{NL}(\omega_i)$, where $\mathbf{P}^{NL}(\omega_i)$ is the nonlinear polarization corresponding to the orders of the power series greater than 1 defined in Section 1.7.2.

Thus the propagation equation of each interacting wave ω_i is (Bloembergen, 1965)

$$\nabla x \nabla x \mathbf{E}(\omega_i) = (\omega_i^2/c^2)\varepsilon(\omega_i)\mathbf{E}(\omega_i) + \omega_i^2 \mu_0 \mathbf{P}^{NL}(\omega_i). \tag{1.7.3.19}$$

The γ propagation equations are coupled by $\mathbf{P}^{NL}(\omega_i)$:

(1) for a three-wave interaction, $\gamma = 3$,

$$\mathbf{P}^{NL}(\omega_1) = \mathbf{P}^{(2)}(\omega_1) = \varepsilon_0 \chi^{(2)}(\omega_1 = \omega_3 - \omega_2) \cdot \mathbf{E}(\omega_3) \otimes \mathbf{E}^*(\omega_2),$$
$$\mathbf{P}^{NL}(\omega_2) = \mathbf{P}^{(2)}(\omega_2) = \varepsilon_0 \chi^{(2)}(\omega_2 = \omega_3 - \omega_1) \cdot \mathbf{E}(\omega_3) \otimes \mathbf{E}^*(\omega_1),$$
$$\mathbf{P}^{NL}(\omega_3) = \mathbf{P}^{(2)}(\omega_3) = \varepsilon_0 \chi^{(2)}(\omega_3 = \omega_1 + \omega_2) \cdot \mathbf{E}(\omega_1) \otimes \mathbf{E}^*(\omega_2);$$

(2) for a four-wave interaction

$$\mathbf{P}^{NL}(\omega_1) = \mathbf{P}^{(3)}(\omega_1) = \varepsilon_0 \chi^{(3)}(\omega_1 = \omega_4 - \omega_2 - \omega_3) \cdot \mathbf{E}(\omega_4) \otimes \mathbf{E}^*(\omega_2) \otimes \mathbf{E}^*(\omega_3),$$
$$\mathbf{P}^{NL}(\omega_2) = \mathbf{P}^{(3)}(\omega_2) = \varepsilon_0 \chi^{(3)}(\omega_2 = \omega_4 - \omega_1 - \omega_3) \cdot \mathbf{E}(\omega_4) \otimes \mathbf{E}^*(\omega_1) \otimes \mathbf{E}^*(\omega_3),$$
$$\mathbf{P}^{NL}(\omega_3) = \mathbf{P}^{(3)}(\omega_3) = \varepsilon_0 \chi^{(3)}(\omega_3 = \omega_4 - \omega_1 - \omega_2) \cdot \mathbf{E}(\omega_4) \otimes \mathbf{E}^*(\omega_1) \otimes \mathbf{E}^*(\omega_2)$$
$$\mathbf{P}^{NL}(\omega_4) = \mathbf{P}^{(3)}(\omega_4) = \varepsilon_0 \chi^{(3)}(\omega_4 = \omega_1 + \omega_2 + \omega_3) \cdot \mathbf{E}(\omega_1) \otimes \mathbf{E}(\omega_2) \otimes \mathbf{E}(\omega_3).$$

The complex conjugates $\mathbf{E}^*(\omega_1)$ come from the relation $\mathbf{E}^*(\omega_i) = \mathbf{E}(-\omega_i)$.

We consider the plane wave, (1.7.3.3), as a solution of (1.7.3.19), and we assume that all the interacting waves propagate in the same direction Z. Each linearly polarized plane wave corresponds to an eigen mode $\mathbf{E}^+$ or $\mathbf{E}^-$ defined above. For the usual case of beams with a finite transversal profile and when Z is along a direction where the double-refraction angles can be nonzero, *i.e.* out of the principal axes of the index surface, it is necessary to specify a frame for each interacting wave in order to calculate the corresponding powers as a function of Z: the coordinates linked to the wave at ω_i are written (X_i, Y_i, Z), which can be relative to the mode (+) or (−). The systems are then linked by the double-refraction angles ρ: according to Fig. 1.7.3.1, we have $X_j^+ = X_i^+ + Z\tan[\rho^+(\omega_j) - \rho^+(\omega_i)]$, $Y_j^+ = Y_i^+$ for two waves (+) with $\rho^+(\omega_j) > \rho^+(\omega_i)$, and $X_j^- = X_i^-$, $Y_j^- = Y_i^- + Z\tan[\rho^-(\omega_j) - \rho^-(\omega_i)]$ for two waves (−) with $\rho^-(\omega_j) > \rho^-(\omega_i)$.

The presence of $\mathbf{P}^{NL}(\omega_i)$ in equations (1.7.3.19) leads to a variation of the γ amplitudes $E(\omega_i)$ with Z. In order to establish the equations of evolution of the wave amplitudes, we assume that their variations are small over one wavelength λ_i, which is usually true. Thus we can state

$$\frac{1}{k(\omega_i)}\left|\frac{\partial E(\omega_i, X_i, Y_i, Z)}{\partial Z}\right| \ll \left|E(\omega_i, X_i, Y_i, Z)\right| \text{ or}$$
$$\left|\frac{\partial^2 E(\omega_i, X_i, Y_i, Z)}{\partial Z^2}\right| \ll k(\omega_i)\left|\frac{\partial E(\omega_i, X_i, Y_i, Z)}{\partial Z}\right|. \tag{1.7.3.20}$$

This is called the slowly varying envelope approximation.

Stating (1.7.3.20), the wave equation (1.7.3.19) for a forward propagation of a plane wave leads to

$$\frac{\partial E(\omega_i, X_i, Y_i, Z)}{\partial Z} = j\mu_0 \frac{\omega_i^2}{2k(\omega_i)\cos^2\rho(\omega_i)} \mathbf{e}(\omega_i) \cdot \mathbf{P}^{NL}(\omega_i, X_i, Y_i, Z) \times \exp[-jk(\omega_i)Z]. \tag{1.7.3.21}$$

We choose the optical frame (x, y, z) for the calculation of all the scalar products $\mathbf{e}(\omega_i) \cdot \mathbf{P}^{NL}(\omega_i)$, the electric susceptibility tensors being known in this frame.

For a three-wave interaction, (1.7.3.21) leads to

$$\frac{\partial E_1(X_1, Y_1, Z)}{\partial Z} = j\kappa_1\left[\mathbf{e}_1 \cdot \varepsilon_0 \chi^{(2)}(\omega_1 = \omega_3 - \omega_2) \cdot \mathbf{e}_3 \otimes \mathbf{e}_2\right] \times E_3(X_3, Y_3, Z)E_2^*(X_2, Y_2, Z)\exp(j\Delta kZ)$$
$$\frac{\partial E_2(X_2, Y_2, Z)}{\partial Z} = j\kappa_2\left[\mathbf{e}_2 \cdot \varepsilon_0 \chi^{(2)}(\omega_2 = \omega_3 - \omega_1) \cdot \mathbf{e}_3 \otimes \mathbf{e}_1\right] \times E_3(X_3, Y_3, Z)E_1^*(X_1, Y_1, Z)\exp(j\Delta kZ)$$
$$\frac{\partial E_3(X_3, Y_3, Z)}{\partial Z} = j\kappa_3\left[\mathbf{e}_3 \cdot \varepsilon_0 \chi^{(2)}(\omega_3 = \omega_1 + \omega_2) \cdot \mathbf{e}_1 \otimes \mathbf{e}_2\right] \times E_1(X_1, Y_1, Z)E_2(X_2, Y_2, Z)\exp(-j\Delta kZ), \tag{1.7.3.22}$$

with $\mathbf{e}_i = \mathbf{e}(\omega_i)$, $E_i(X_i, Y_i, Z_i) = E(\omega_i, X_i, Y_i, Z)$, $\kappa_i = (\mu_o\omega_i^2)/[2k(\omega_i)\cos^2\rho(\omega_i)]$ and $\Delta k = k(\omega_3) - [k(\omega_1) + k(\omega_2)]$, called the phase mismatch. We take by convention $\omega_1 < \omega_2$ $(< \omega_3)$.

If ABDP relations, defined in Section 1.7.2.2.1, are verified, then the three tensorial contractions in equations (1.7.3.22) are equal to the same quantity, which we write $\varepsilon_0\chi^{(2)}_{\rm eff}$, where $\chi^{(2)}_{\rm eff}$ is called the effective coefficient:

$$\begin{aligned}\chi^{(2)}_{\rm eff} &= \mathbf{e}_1\cdot\chi^{(2)}(\omega_1=\omega_3-\omega_2)\cdot\mathbf{e}_3\otimes\mathbf{e}_2\\ &= \mathbf{e}_2\cdot\chi^{(2)}(\omega_2=\omega_3-\omega_1)\cdot\mathbf{e}_3\otimes\mathbf{e}_1\\ &= \mathbf{e}_3\cdot\chi^{(2)}(\omega_3=\omega_1+\omega_2)\cdot\mathbf{e}_1\otimes\mathbf{e}_2.\end{aligned}\tag{1.7.3.23}$$

The same considerations lead to the same kind of equations for a four-wave interaction:

$$\begin{aligned}\frac{\partial E_1(X_1,Y_1,Z)}{\partial Z} &= j\kappa_1\varepsilon_0\chi^{(3)}_{\rm eff}E_4(X_4,Y_4,Z)E_2^*(X_2,Y_2,Z)\\ &\quad\times E_3^*(X_3,Y_3,Z)\exp(j\Delta kZ)\\ \frac{\partial E_2(X_2,Y_2,Z)}{\partial Z} &= j\kappa_2\varepsilon_0\chi^{(3)}_{\rm eff}E_4(X_4,Y_4,Z)E_1^*(X_1,Y_1,Z)\\ &\quad\times E_3^*(X_3,Y_3,Z)\exp(j\Delta kZ)\\ \frac{\partial E_3(X_3,Y_3,Z)}{\partial Z} &= j\kappa_3\varepsilon_0\chi^{(3)}_{eff}E_4(X_4,Y_4,Z)E_1^*(X_1,Y_1,Z)\\ &\quad\times E_2^*(X_2,Y_2,Z)\exp(j\Delta kZ)\\ \frac{\partial E_4(X_4,Y_4,Z)}{\partial Z} &= j\kappa_4\varepsilon_0\chi^{(3)}_{eff}E_1(X_1,Y_1,Z)E_2(X_2,Y_2,Z)\\ &\quad\times E_3(X_3,Y_3,Z)\exp(-j\Delta kZ).\end{aligned}\tag{1.7.3.24}$$

The conventions of notation are the same as previously and the phase mismatch is $\Delta k = k(\omega_4)-[k(\omega_1)+k(\omega_2)+k(\omega_3)]$. The effective coefficient is

$$\begin{aligned}\chi^{(3)}_{\rm eff} &= \mathbf{e}_1\cdot\chi^{(3)}(\omega_1=\omega_4-\omega_2-\omega_3)\cdot\mathbf{e}_4\otimes\mathbf{e}_2\otimes\mathbf{e}_3\\ &= \mathbf{e}_2\cdot\chi^{(3)}(\omega_2=\omega_4-\omega_1-\omega_3)\cdot\mathbf{e}_4\otimes\mathbf{e}_1\otimes\mathbf{e}_3\\ &= \mathbf{e}_3\cdot\chi^{(3)}(\omega_3=\omega_4-\omega_1-\omega_2)\cdot\mathbf{e}_4\otimes\mathbf{e}_1\otimes\mathbf{e}_2\\ &= \mathbf{e}_4\cdot\chi^{(3)}(\omega_4=\omega_1+\omega_2+\omega_3)\cdot\mathbf{e}_1\otimes\mathbf{e}_2\otimes\mathbf{e}_3.\end{aligned}\tag{1.7.3.25}$$

Expressions (1.7.3.23) for $\chi^{(2)}_{\rm eff}$ and (1.7.3.25) for $\chi^{(3)}_{\rm eff}$ can be condensed by introducing adequate third- and fourth-rank tensors to be contracted, respectively, with $\chi^{(2)}$ and $\chi^{(3)}$. For example, $\chi^{(2)}_{\rm eff}=\chi^{(2)}\cdot e_3\otimes e_1\otimes e_2$ or $\chi^{(3)}_{\rm eff}=\chi^{(3)}\cdot e_4\otimes e_1\otimes e_2\otimes e_3$, and similar expressions. By substituting (1.7.3.8) in (1.7.3.22), we obtain the derivatives of Manley–Rowe relations (1.7.2.40) $\partial N(\omega_3,Z)/\partial Z=-\partial N(\omega_k,Z)/\partial Z$ $(k=1,2)$ for a three-wave mixing, where $N(\omega_i,Z)$ is the Z photon flow. Identically with (1.7.3.24), we have $\partial N(\omega_4,Z)/\partial Z=-\partial N(\omega_k,Z)/\partial Z$ $(k=1,2,3)$ for a four-wave mixing.

In the general case, the nonlinear polarization wave and the generated wave travel at different phase velocities, $(\omega_1+\omega_2)/[k(\omega_1)+k(\omega_2)]$ and $\omega_3/[k(\omega_3)]$, respectively, because of the frequency dispersion of the refractive indices in the crystal. Then the work per unit time $W(\omega_i)$, given in (1.7.2.39), which is done on the generated wave $\mathbf{E}(\omega_i,Z)$ by the nonlinear polarization $\mathbf{P}^{NL}(\omega_i,Z)$, alternates in sign for each phase shift of π during the Z-propagation, which leads to a reversal of the energy flow (Bloembergen, 1965). The length leading to the phase shift of π is called the coherence length, $L_c=\pi/\Delta k$, where Δk is the phase mismatch given by (1.7.3.22) or (1.7.3.24).

1.7.3.2.2. *Phase matching*

The transfer of energy between the waves is maximum for $\Delta k=0$, which defines phase matching: the energy flow does not alternate in sign and the generated field grows continuously. Note that a condition relative to the phases $\Phi(\omega_i,Z)$ also exists: the work of $\mathbf{P}^{NL}(\omega_i,Z)$ on $\mathbf{E}(\omega_i,Z)$ is maximum if these two waves are $\pi/2$ out of phase, that is to say if $\Delta kZ+\Delta\Phi(Z)=\pi/2$, where $\Delta\Phi(Z)=\Phi(\omega_3,Z)-[\Phi(\omega_1,Z)+\Phi(\omega_2,Z)]$; thus in the case of phase matching, the phase relation is $\Phi(\omega_3,Z)=\Phi(\omega_1,Z)+\Phi(\omega_2,Z)+\pi/2$ (Armstrong *et al.*, 1962). The complete initial phase matching is necessarily achieved when at least one wave among all the interacting waves is not incident but is generated inside the nonlinear crystal: in this case, its initial phase is locked on the good one. Phase matching is usually realized by the matching of the refractive indices using birefringence of anisotropic media as it is studied here. From the point of view of the quantum theory of light, the phase matching of the waves corresponds to the total photon-momentum conservation *i.e.*

$$\sum_{i=1}^{\gamma-1}\hbar k(\omega_i)=\hbar k(\omega_\gamma)\tag{1.7.3.26}$$

with $\gamma=3$ for a three-photon interaction and $\gamma=4$ for a four-photon interaction.

According to (1.7.3.4), the phase-matching condition (1.7.3.26) is expressed as a function of the refractive indices in the direction of propagation considered (θ,φ); for an interaction where the γ wavevectors are collinear, it is written

$$\sum_{i=1}^{\gamma-1}\omega_i n(\omega_i,\theta,\varphi)=\omega_\gamma n(\omega_\gamma,\theta,\varphi)\tag{1.7.3.27}$$

with

$$\sum_{i=1}^{\gamma-1}\omega_i=\omega_\gamma.\tag{1.7.3.28}$$

(1.7.3.28) is the relation of the energy conservation.

The efficiency of a nonlinear crystal directly depends on the existence of phase-matching directions. We shall see by considering in detail the effective coefficient that phase matching is a necessary but insufficient condition for the best expression of the nonlinear optical properties.

In an hypothetical non-dispersive medium $[\partial n(\omega)/\partial\omega=0]$, (1.7.3.27) is always verified for each of the eigen refractive indices n^+ or n^-; then any direction of propagation is a phase-matching direction. In a dispersive medium, phase matching can be achieved only if the direction of propagation has a birefringence which compensates the dispersion. Except for a propagation along the optic axis, there are two possible values, n^+ and n^- given by (1.7.3.6), for each of the three or four refractive indices involved in the phase-matching relations, that is to say 2^3 or 2^4 possible combinations of refractive indices for a three-wave or a four-wave process, respectively.

For a three-wave process, only three combinations among the 2^3 are compatible with the dispersion in frequency (1.7.3.7) and with the momentum and energy conservations (1.7.3.27) and (1.7.3.28). Thus the phase matching of a

Table 1.7.3.1. *Correspondence between the phase-matching relations, the configurations of polarization and the types according to the sum- and difference-frequency generation processes SFG ($\omega_3=\omega_1+\omega_2$), DFG ($\omega_1=\omega_3-\omega_2$) and DFG ($\omega_2=\omega_3-\omega_1$)*

$\mathbf{e}^\pm$ are the unit electric field vectors relative to the refractive indices $n^\pm$ in the phase-matching direction (Boulanger & Marnier, 1991).

	Configurations of polarization			Types of interaction		
Phase-matching relations	ω_3	ω_1	ω_2	SFG (ω_3)	DFG (ω_1)	DFG (ω_2)
$\omega_3n_3^-=\omega_1n_1^+=\omega_2n_2^+$	$\mathbf{e}^-$	$\mathbf{e}^+$	$\mathbf{e}^+$	I	II	III
$\omega_3n_3^-=\omega_1n_1^-=\omega_2n_2^+$	$\mathbf{e}^-$	$\mathbf{e}^-$	$\mathbf{e}^+$	II	III	I
$\omega_3n_3^-=\omega_1n_1^+=\omega_2n_2^-$	$\mathbf{e}^-$	$\mathbf{e}^+$	$\mathbf{e}^-$	III	I	II

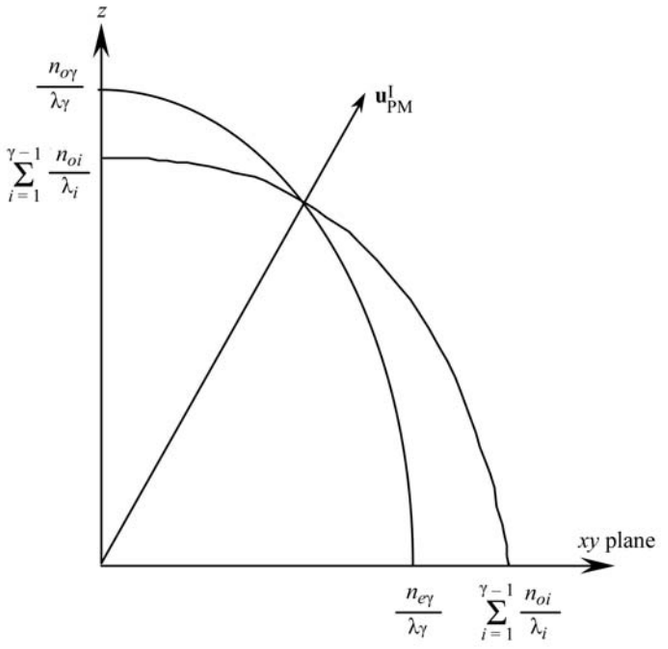

Fig. 1.7.3.4. Index surface sections in a plane containing the optic axis z of a negative uniaxial crystal allowing collinear type-I phase matching for SFG ($\omega_3 = \omega_1 + \omega_2$), $\gamma = 3$, or for SFG ($\omega_4 = \omega_1 + \omega_2 + \omega_3$), $\gamma = 4$. $\mathbf{u}^{\mathrm{I}}_{\mathrm{PM}}$ is the corresponding phase-matching direction.

three-wave interaction is allowed for three configurations of polarization given in Table 1.7.3.1.

The designation of the type of phase matching, I, II or III, is defined according to the polarization states at the frequencies which are added or subtracted. Type I characterizes interactions for which these two waves are identically polarized; the two corresponding polarizations are different for types II and III. Note that each phase-matching relation corresponds to one sum-frequency generation SFG ($\omega_3 = \omega_1 + \omega_2$) and two difference-frequency generation processes, DFG ($\omega_1 = \omega_3 - \omega_2$) and DFG ($\omega_2 = \omega_3 - \omega_1$). Types II and III are equivalent for SHG because $\omega_1 = \omega_2$.

For a four-wave process, only seven combinations of refractive indices allow phase matching in the case of normal dispersion; they are given in Table 1.7.3.2 with the corresponding configurations of polarization and types of SFG and DFG.

The convention of designation of the types is the same as for three-wave interactions for the situations where one polarization state is different from the three others, leading to the types I, II, III and IV. The criterion corresponding to type I cannot be applied to the three other phase-matching relations where two waves have the same polarization state, different from the two others. In this case, it is convenient to refer to each phase-matching relation by the same roman numeral, but with a different index: V^i, VI^i and VII^i, with the index $i = 1, 2, 3, 4$ corresponding to the index of the frequency generated by the SFG or DFG. For THG ($\omega_1 = \omega_2 = \omega_3$), types II, III and IV are equivalent, and so are types V^4, VI^4 and VII^4.

The index surface allows the geometrical determination of the phase-matching directions, which depend on the relative ellipticity of the internal (−) and external (+) sheets divided by the corresponding wavelengths: according to Tables 1.7.3.1 and 1.7.3.2 the directions are given by the intersection of the internal sheet of the lowest wavelength $[n^-(\lambda_\gamma, \theta, \varphi)]/(\lambda_\gamma)$ with a linear combination of the internal and external sheets at the other frequencies $\sum_{i=1}^{\gamma-1}[n^{\pm}(\lambda_i, \theta, \varphi)]/(\lambda_i)$. The existence and loci of these intersections depend on specific inequalities between the principal refractive indices at the different wavelengths. Note that independently of phase-matching considerations, normal dispersion and energy conservation impose $\sum_{i=1}^{\gamma-1}[n_a(\lambda_i)]/(\lambda_i) < [n_a(\lambda_\gamma)]/(\lambda_\gamma)$ with $a = x, y, z$.

1.7.3.2.2.1. *Cubic crystals*

There is no possibility of collinear phase matching in a dispersive cubic crystal because of the absence of birefringence. In a hypothetical non-dispersive anaxial crystal, the 2^3 three-wave and 2^4 four-wave phase-matching configurations would be allowed in any direction of propagation.

1.7.3.2.2.2. *Uniaxial crystals*

The configurations of polarization in terms of ordinary and extraordinary waves depend on the optic sign of the phase-matching direction with the convention given in Section 1.7.3.1: Tables 1.7.3.1 and 1.7.3.2 must be read by substituting (+, −) by (e, o) for a positive crystal and by (o, e) for a negative one.

Because of the symmetry of the index surface, all the phase-matching directions for a given type describe a cone with the optic axis as a revolution axis. Note that the previous comment on the anaxial class is valid for a propagation along the optic axis ($n_o = n_e$).

Fig. 1.7.3.4 shows the example of negative uniaxial crystals ($n_o > n_e$) like β-BaB_2O_4 (BBO) and KH_2PO_4 (KDP).

From Fig. 1.7.3.4, it clearly appears that the intersection of the sheets is possible only if $(n_{e_\gamma})/(\lambda_\gamma) < \sum_{i=1}^{\gamma-1}(n_{o_i})/(\lambda_i)$ $[< (n_{o_\gamma})/(\lambda_\gamma)]$ with $\gamma = 3$ for a three-wave process and $\gamma = 4$ for a four-wave one. The same considerations can be made for the positive sign and for all the other types of phase matching. There are different situations of inequalities allowing zero, one or several types: Table 1.7.3.3 gives the five possible situations for the three-wave interactions and Table 1.7.3.4 the 19 situations for the four-wave processes.

1.7.3.2.2.3. *Biaxial crystals*

The situation of biaxial crystals is more complicated, because the two sheets that must intersect are both elliptical in several cases. For a given interaction, all the phase-matching directions generate a complicated cone which joins two directions in the principal planes; the possible loci a, b, c, d are shown on the stereographic projection given in Fig. 1.7.3.5.

The basic inequalities of normal dispersion (1.7.3.7) forbid collinear phase matching for all the directions of propagation located between two optic axes at the two frequencies concerned.

Table 1.7.3.2. *Correspondence between the phase-matching relations, the configurations of polarization and the types according to SFG ($\omega_4 = \omega_1 + \omega_2 + \omega_3$), DFG ($\omega_1 = \omega_4 - \omega_2 - \omega_3$), DFG ($\omega_2 = \omega_4 - \omega_1 - \omega_3$) and DFG ($\omega_3 = \omega_4 - \omega_1 - \omega_2$) (Boulanger et al., 1993)*

	Configurations of polarization				Types of interaction			
Phase-matching relations	ω_4	ω_1	ω_2	ω_3	SFG (ω_4)	DFG (ω_1)	DFG (ω_2)	DFG (ω_3)
$\omega_4 n_4^- = \omega_1 n_1^+ + \omega_2 n_2^+ + \omega_3 n_3^+$	$\mathbf{e}^-$	$\mathbf{e}^+$	$\mathbf{e}^+$	$\mathbf{e}^+$	I	II	III	IV
$\omega_4 n_4^- = \omega_1 n_1^- + \omega_2 n_2^- + \omega_3 n_3^+$	$\mathbf{e}^-$	$\mathbf{e}^-$	$\mathbf{e}^-$	$\mathbf{e}^+$	II	III	IV	I
$\omega_4 n_4^- = \omega_1 n_1^- + \omega_2 n_2^+ + \omega_3 n_3^-$	$\mathbf{e}^-$	$\mathbf{e}^-$	$\mathbf{e}^+$	$\mathbf{e}^-$	III	IV	I	II
$\omega_4 n_4^- = \omega_1 n_1^+ + \omega_2 n_2^- + \omega_3 n_3^-$	$\mathbf{e}^-$	$\mathbf{e}^+$	$\mathbf{e}^-$	$\mathbf{e}^-$	IV	I	II	IV
$\omega_4 n_4^- = \omega_1 n_1^- + \omega_2 n_2^+ + \omega_3 n_3^+$	$\mathbf{e}^-$	$\mathbf{e}^-$	$\mathbf{e}^+$	$\mathbf{e}^+$	V^4	V^1	V^2	V^3
$\omega_4 n_4^- = \omega_1 n_1^+ + \omega_2 n_2^- + \omega_3 n_3^+$	$\mathbf{e}^-$	$\mathbf{e}^+$	$\mathbf{e}^-$	$\mathbf{e}^+$	VI^4	VI^1	VI^2	VI^3
$\omega_4 n_4^- = \omega_1 n_1^+ + \omega_2 n_2^+ + \omega_3 n_3^-$	$\mathbf{e}^-$	$\mathbf{e}^+$	$\mathbf{e}^+$	$\mathbf{e}^-$	VII^4	VII^1	VII^2	VII^3

Table 1.7.3.3. *Classes of refractive-index inequalities for collinear phase matching of three-wave interactions in positive and negative uniaxial crystals*

Types I, II and III refer to SFG; the types of the corresponding DFG are given in Table 1.7.3.1 (Fève *et al.*, 1993).

Positive sign ($n_e > n_o$)	Negative sign ($n_o > n_e$)	Types of SFG
$\frac{n_{o3}}{\lambda_3} < \frac{n_{o1}}{\lambda_1} + \frac{n_{e2}}{\lambda_2}; \frac{n_{e1}}{\lambda_1} + \frac{n_{o2}}{\lambda_2}$	$\frac{n_{o1}}{\lambda_1} + \frac{n_{e2}}{\lambda_2}, \frac{n_{e1}}{\lambda_1} + \frac{n_{o2}}{\lambda_2} < \frac{n_{e3}}{\lambda_3}$	I, II, III
$\frac{n_{e1}}{\lambda_1} + \frac{n_{o2}}{\lambda_2} < \frac{n_{o3}}{\lambda_3} < \frac{n_{o1}}{\lambda_1} + \frac{n_{e2}}{\lambda_2}$	$\frac{n_{o1}}{\lambda_1} + \frac{n_{e2}}{\lambda_2} < \frac{n_{e3}}{\lambda_3} < \frac{n_{e1}}{\lambda_1} + \frac{n_{o2}}{\lambda_2}$	I, II
$\frac{n_{o1}}{\lambda_1} + \frac{n_{e2}}{\lambda_2} < \frac{n_{o3}}{\lambda_3} < \frac{n_{e1}}{\lambda_1} + \frac{n_{o2}}{\lambda_2}$	$\frac{n_{e1}}{\lambda_1} + \frac{n_{o2}}{\lambda_2} < \frac{n_{e3}}{\lambda_3} < \frac{n_{o1}}{\lambda_1} + \frac{n_{e2}}{\lambda_2}$	I, III
$\frac{n_{o1}}{\lambda_1} + \frac{n_{e2}}{\lambda_2}, \frac{n_{e1}}{\lambda_1} + \frac{n_{o2}}{\lambda_2} < \frac{n_{o3}}{\lambda_3} < \frac{n_{e_1}}{\lambda_1} + \frac{n_{e2}}{\lambda_2}$	$\frac{n_{o1}}{\lambda_1} + \frac{n_{e2}}{\lambda_2}, \frac{n_{e1}}{\lambda_1} + \frac{n_{o2}}{\lambda_2} < \frac{n_{e3}}{\lambda_3} < \frac{n_{o_1}}{\lambda_1} + \frac{n_{o2}}{\lambda_2}$	I
$\frac{n_{e_1}}{\lambda_1} + \frac{n_{e2}}{\lambda_2} < \frac{n_{o3}}{\lambda_3}$	$\frac{n_{o_1}}{\lambda_1} + \frac{n_{o2}}{\lambda_2} < \frac{n_{e3}}{\lambda_3}$	None

Table 1.7.3.4. *Classes of refractive-index inequalities for collinear phase matching of four-wave interactions in positive ($n_a = n_e, n_b = n_o$) and negative ($n_a = n_o, n_b = n_e$) uniaxial crystals with $(n_{b4}/\lambda_4) < (n_{a1}/\lambda_1) + (n_{a2}/\lambda_2) + (n_{a3}/\lambda_3)$*

If this inequality is not verified, no phase matching is allowed. The types of phase matching refer to SFG; the types of the corresponding DFG are given in Table 1.7.3.2 (Fève, 1994).

Positive sign ($n_e > n_o$)	Negative sign ($n_o > n_e$)	Types of SFG
$\frac{n_{a1}}{\lambda_1} + \frac{n_{a2}}{\lambda_2} + \frac{n_{b3}}{\lambda_3}, \frac{n_{a1}}{\lambda_1} + \frac{n_{b2}}{\lambda_2} + \frac{n_{a3}}{\lambda_3}, \frac{n_{b1}}{\lambda_1} + \frac{n_{a2}}{\lambda_2} + \frac{n_{a3}}{\lambda_3} < \frac{n_{b4}}{\lambda_4}$		I
$\frac{n_{a1}}{\lambda_1} + \frac{n_{a2}}{\lambda_2} + \frac{n_{b3}}{\lambda_3}, \frac{n_{a1}}{\lambda_1} + \frac{n_{b2}}{\lambda_2} + \frac{n_{a3}}{\lambda_3} < \frac{n_{b4}}{\lambda_4} < \frac{n_{b1}}{\lambda_1} + \frac{n_{a2}}{\lambda_2} + \frac{n_{a3}}{\lambda_3}$		I, V^4
$\frac{n_{a1}}{\lambda_1} + \frac{n_{a2}}{\lambda_2} + \frac{n_{b3}}{\lambda_3}, \frac{n_{b1}}{\lambda_1} + \frac{n_{a2}}{\lambda_2} + \frac{n_{a3}}{\lambda_3} < \frac{n_{b4}}{\lambda_4} < \frac{n_{a1}}{\lambda_1} + \frac{n_{b2}}{\lambda_2} + \frac{n_{a3}}{\lambda_3}$		I, VI^4
$\frac{n_{a1}}{\lambda_1} + \frac{n_{b2}}{\lambda_2} + \frac{n_{a3}}{\lambda_3}, \frac{n_{b1}}{\lambda_1} + \frac{n_{a2}}{\lambda_2} + \frac{n_{a3}}{\lambda_3} < \frac{n_{b4}}{\lambda_4} < \frac{n_{a1}}{\lambda_1} + \frac{n_{a2}}{\lambda_2} + \frac{n_{b3}}{\lambda_3}$		I, VII^4
$\frac{n_{a1}}{\lambda_1} + \frac{n_{a2}}{\lambda_2} + \frac{n_{b3}}{\lambda_3} < \frac{n_{b4}}{\lambda_4} < \frac{n_{a1}}{\lambda_1} + \frac{n_{b2}}{\lambda_2} + \frac{n_{a3}}{\lambda_3}, \frac{n_{b1}}{\lambda_1} + \frac{n_{a2}}{\lambda_2} + \frac{n_{a3}}{\lambda_3}$	$\frac{n_{b1}}{\lambda_1} + \frac{n_{b2}}{\lambda_2} + \frac{n_{a3}}{\lambda_3} < \frac{n_{b4}}{\lambda_4}$	I, V^4, VI^4
	$\frac{n_{b4}}{\lambda_4} < \frac{n_{b1}}{\lambda_1} + \frac{n_{b2}}{\lambda_2} + \frac{n_{a3}}{\lambda_3}$	I, II, V^4, VI^4
$\frac{n_{a1}}{\lambda_1} + \frac{n_{b2}}{\lambda_2} + \frac{n_{a3}}{\lambda_3} < \frac{n_{b4}}{\lambda_4} < \frac{n_{a1}}{\lambda_1} + \frac{n_{a2}}{\lambda_2} + \frac{n_{b3}}{\lambda_3}, \frac{n_{b1}}{\lambda_1} + \frac{n_{a2}}{\lambda_2} + \frac{n_{a3}}{\lambda_3}$	$\frac{n_{b1}}{\lambda_1} + \frac{n_{a2}}{\lambda_2} + \frac{n_{b3}}{\lambda_3} < \frac{n_{b4}}{\lambda_4}$	I, V^4, VII^4
	$\frac{n_{b4}}{\lambda_4} < \frac{n_{b1}}{\lambda_1} + \frac{n_{a2}}{\lambda_2} + \frac{n_{b3}}{\lambda_3}$	I, III, V^4, VII^4
$\frac{n_{b1}}{\lambda_1} + \frac{n_{a2}}{\lambda_2} + \frac{n_{a3}}{\lambda_3} < \frac{n_{b4}}{\lambda_4} < \frac{n_{a1}}{\lambda_1} + \frac{n_{b2}}{\lambda_2} + \frac{n_{a3}}{\lambda_3}, \frac{n_{a1}}{\lambda_1} + \frac{n_{a2}}{\lambda_2} + \frac{n_{b3}}{\lambda_3}$	$\frac{n_{a1}}{\lambda_1} + \frac{n_{b2}}{\lambda_2} + \frac{n_{b3}}{\lambda_3} < \frac{n_{b4}}{\lambda_4}$	I, VI^4, VII^4
	$\frac{n_{b4}}{\lambda_4} < \frac{n_{a1}}{\lambda_1} + \frac{n_{b2}}{\lambda_2} + \frac{n_{b3}}{\lambda_3}$	I, IV, VI^4, VII^4
$\frac{n_{b4}}{\lambda_4} < \frac{n_{a1}}{\lambda_1} + \frac{n_{a2}}{\lambda_2} + \frac{n_{b3}}{\lambda_3}, \frac{n_{a1}}{\lambda_1} + \frac{n_{b2}}{\lambda_2} + \frac{n_{a3}}{\lambda_3}, \frac{n_{b1}}{\lambda_1} + \frac{n_{a2}}{\lambda_2} + \frac{n_{a3}}{\lambda_3}$	$\frac{n_{b1}}{\lambda_1} + \frac{n_{b2}}{\lambda_2} + \frac{n_{a3}}{\lambda_3}, \frac{n_{b1}}{\lambda_1} + \frac{n_{a2}}{\lambda_2} + \frac{n_{b3}}{\lambda_3}, \frac{n_{a1}}{\lambda_1} + \frac{n_{b2}}{\lambda_2} + \frac{n_{b3}}{\lambda_3} < \frac{n_{b4}}{\lambda_4}$	I, V^4, VI^4, VII^4
	$\frac{n_{a1}}{\lambda_1} + \frac{n_{b2}}{\lambda_2} + \frac{n_{b3}}{\lambda_3}, \frac{n_{b1}}{\lambda_1} + \frac{n_{a2}}{\lambda_2} + \frac{n_{b3}}{\lambda_3} < \frac{n_{b4}}{\lambda_4} < \frac{n_{b1}}{\lambda_1} + \frac{n_{b2}}{\lambda_2} + \frac{n_{a3}}{\lambda_3}$	I, II, V^4, VI^4, VII^4
	$\frac{n_{a1}}{\lambda_1} + \frac{n_{b2}}{\lambda_2} + \frac{n_{b3}}{\lambda_3}, \frac{n_{b1}}{\lambda_1} + \frac{n_{b2}}{\lambda_2} + \frac{n_{a3}}{\lambda_3} < \frac{n_{b4}}{\lambda_4} < \frac{n_{b1}}{\lambda_1} + \frac{n_{a2}}{\lambda_2} + \frac{n_{b3}}{\lambda_3}$	I, III, V^4, VI^4, VII^4
	$\frac{n_{b1}}{\lambda_1} + \frac{n_{a2}}{\lambda_2} + \frac{n_{b3}}{\lambda_3}, \frac{n_{b1}}{\lambda_1} + \frac{n_{b2}}{\lambda_2} + \frac{n_{a3}}{\lambda_3} < \frac{n_{b4}}{\lambda_4} < \frac{n_{a1}}{\lambda_1} + \frac{n_{b2}}{\lambda_2} + \frac{n_{b3}}{\lambda_3}$	I, IV, V^4, VI^4, VII^4
	$\frac{n_{a1}}{\lambda_1} + \frac{n_{b2}}{\lambda_2} + \frac{n_{b3}}{\lambda_3} < \frac{n_{b4}}{\lambda_4} < \frac{n_{b1}}{\lambda_1} + \frac{n_{a2}}{\lambda_2} + \frac{n_{b3}}{\lambda_3}, \frac{n_{b1}}{\lambda_1} + \frac{n_{b2}}{\lambda_2} + \frac{n_{a3}}{\lambda_3}$	I, II, III, V^4, VI^4, VII^4
	$\frac{n_{b1}}{\lambda_1} + \frac{n_{a2}}{\lambda_2} + \frac{n_{b3}}{\lambda_3} < \frac{n_{b4}}{\lambda_4} < \frac{n_{a1}}{\lambda_1} + \frac{n_{b2}}{\lambda_2} + \frac{n_{b3}}{\lambda_3}, \frac{n_{b1}}{\lambda_1} + \frac{n_{b2}}{\lambda_2} + \frac{n_{a3}}{\lambda_3}$	I, II, IV, V^4, VI^4, VII^4
	$\frac{n_{b1}}{\lambda_1} + \frac{n_{b2}}{\lambda_2} + \frac{n_{a3}}{\lambda_3} < \frac{n_{b4}}{\lambda_4} < \frac{n_{a1}}{\lambda_1} + \frac{n_{b2}}{\lambda_2} + \frac{n_{b3}}{\lambda_3}, \frac{n_{b1}}{\lambda_1} + \frac{n_{a2}}{\lambda_2} + \frac{n_{b3}}{\lambda_3}$	I, III, IV, V^4, VI^4, VII^4
	$\frac{n_{b4}}{\lambda_4} < \frac{n_{a1}}{\lambda_1} + \frac{n_{b2}}{\lambda_2} + \frac{n_{b3}}{\lambda_3}, \frac{n_{b1}}{\lambda_1} + \frac{n_{a2}}{\lambda_2} + \frac{n_{b3}}{\lambda_3}, \frac{n_{b1}}{\lambda_1} + \frac{n_{b2}}{\lambda_2} + \frac{n_{a3}}{\lambda_3}$	All

Table 1.7.3.5. *Refractive-index conditions that determine collinear phase-matching loci in the principal planes of positive and negative biaxial crystals for three-wave SFG*

a, *b*, *c*, *d* refer to the areas given in Fig. 1.7.3.5. The types corresponding to the different DFGs are given in Table 1.7.3.1 (Fève *et al.*, 1993).

Types of SFG	Phase-matching loci in the principal planes	Inequalities determining three-wave collinear phase matching in biaxial crystals	
		Positive biaxial crystal	Negative biaxial crystal
		$n_x(\omega_i) < n_y(\omega_i) < n_z(\omega_i)$	$n_x(\omega_i) > n_y(\omega_i) > n_z(\omega_i)$
Type I	*a*	$\frac{n_{x3}}{\lambda_3} < \frac{n_{y1}}{\lambda_1} + \frac{n_{y2}}{\lambda_2} < \frac{n_{z3}}{\lambda_3}$	$\frac{n_{x1}}{\lambda_1} + \frac{n_{x2}}{\lambda_2} > \frac{n_{y3}}{\lambda_3} > \frac{n_{z1}}{\lambda_1} + \frac{n_{z2}}{\lambda_2}$
	b	$\frac{n_{x1}}{\lambda_1} + \frac{n_{x2}}{\lambda_2} < \frac{n_{y3}}{\lambda_3} < \frac{n_{z1}}{\lambda_1} + \frac{n_{z2}}{\lambda_2}$	$\frac{n_{x3}}{\lambda_3} > \frac{n_{y1}}{\lambda_1} + \frac{n_{y2}}{\lambda_2} > \frac{n_{z3}}{\lambda_3}$
	c	$\frac{n_{x3}}{\lambda_3} < \frac{n_{z1}}{\lambda_1} + \frac{n_{z2}}{\lambda_2} < \frac{n_{y3}}{\lambda_3}$	$\frac{n_{x1}}{\lambda_1} + \frac{n_{x2}}{\lambda_2} > \frac{n_{z3}}{\lambda_3} > \frac{n_{y1}}{\lambda_1} + \frac{n_{y2}}{\lambda_2}$
	d	$\frac{n_{y1}}{\lambda_1} + \frac{n_{y2}}{\lambda_2} < \frac{n_{x3}}{\lambda_3} < \frac{n_{z1}}{\lambda_1} + \frac{n_{z2}}{\lambda_2}$	$\frac{n_{y3}}{\lambda_3} > \frac{n_{x1}}{\lambda_1} + \frac{n_{x2}}{\lambda_2} > \frac{n_{z3}}{\lambda_3}$
Type II	*a*	$\frac{n_{x3}}{\lambda_3} < \frac{n_{x1}}{\lambda_1} + \frac{n_{y2}}{\lambda_2}; \frac{n_{z1}}{\lambda_1} + \frac{n_{y2}}{\lambda_2} < \frac{n_{z3}}{\lambda_3}$	$\frac{n_{y1}}{\lambda_1} + \frac{n_{x2}}{\lambda_2} > \frac{n_{y3}}{\lambda_3} > \frac{n_{y1}}{\lambda_1} + \frac{n_{z2}}{\lambda_2}$
	b	$\frac{n_{y1}}{\lambda_1} + \frac{n_{x2}}{\lambda_2} > \frac{n_{y3}}{\lambda_3} > \frac{n_{y1}}{\lambda_1} + \frac{n_{z2}}{\lambda_2}$	$\frac{n_{x3}}{\lambda_3} > \frac{n_{x1}}{\lambda_1} + \frac{n_{y2}}{\lambda_2}; \frac{n_{z1}}{\lambda_1} + \frac{n_{y2}}{\lambda_2} > \frac{n_{z3}}{\lambda_3}$
	c	$\frac{n_{x3}}{\lambda_3} < \frac{n_{x1}}{\lambda_1} + \frac{n_{z2}}{\lambda_2}; \frac{n_{y1}}{\lambda_1} + \frac{n_{z2}}{\lambda_2} < \frac{n_{y3}}{\lambda_3}$	$\frac{n_{z1}}{\lambda_1} + \frac{n_{x2}}{\lambda_2} > \frac{n_{z3}}{\lambda_3} > \frac{n_{z1}}{\lambda_1} + \frac{n_{y2}}{\lambda_2}$
	*c**	$\frac{n_{x1}}{\lambda_1} + \frac{n_{z2}}{\lambda_2} < \frac{n_{x3}}{\lambda_3}; \frac{n_{y3}}{\lambda_3} < \frac{n_{y1}}{\lambda_1} + \frac{n_{z2}}{\lambda_2}$	$\frac{n_{z1}}{\lambda_1} + \frac{n_{x2}}{\lambda_2} > \frac{n_{z3}}{\lambda_3} > \frac{n_{z1}}{\lambda_1} + \frac{n_{y2}}{\lambda_2}$
	d	$\frac{n_{x1}}{\lambda_1} + \frac{n_{y2}}{\lambda_2} < \frac{n_{x3}}{\lambda_3} < \frac{n_{x1}}{\lambda_1} + \frac{n_{z2}}{\lambda_2}$	$\frac{n_{y3}}{\lambda_3} > \frac{n_{y1}}{\lambda_1} + \frac{n_{x2}}{\lambda_2}; \frac{n_{z1}}{\lambda_1} + \frac{n_{x2}}{\lambda_2} > \frac{n_{z3}}{\lambda_3}$
	*d**	$\frac{n_{x1}}{\lambda_1} + \frac{n_{y2}}{\lambda_2} < \frac{n_{x3}}{\lambda_3} < \frac{n_{x1}}{\lambda_1} + \frac{n_{z2}}{\lambda_2}$	$\frac{n_{y1}}{\lambda_1} + \frac{n_{x2}}{\lambda_2} > \frac{n_{y3}}{\lambda_3}; \frac{n_{z3}}{\lambda_3} > \frac{n_{z1}}{\lambda_1} + \frac{n_{x2}}{\lambda_2}$
Type III	*a*	$\frac{n_{x3}}{\lambda_3} < \frac{n_{y1}}{\lambda_1} + \frac{n_{x2}}{\lambda_2}; \frac{n_{y1}}{\lambda_1} + \frac{n_{z2}}{\lambda_2} < \frac{n_{z3}}{\lambda_3}$	$\frac{n_{x1}}{\lambda_1} + \frac{n_{y2}}{\lambda_2} > \frac{n_{y3}}{\lambda_3} > \frac{n_{z1}}{\lambda_1} + \frac{n_{y2}}{\lambda_2}$
	b	$\frac{n_{x1}}{\lambda_1} + \frac{n_{y2}}{\lambda_2} < \frac{n_{y3}}{\lambda_3} < \frac{n_{z1}}{\lambda_1} + \frac{n_{y2}}{\lambda_2}$	$\frac{n_{x3}}{\lambda_3} > \frac{n_{y1}}{\lambda_1} + \frac{n_{x2}}{\lambda_2}; \frac{n_{y1}}{\lambda_1} + \frac{n_{z2}}{\lambda_2} > \frac{n_{z3}}{\lambda_3}$
	c	$\frac{n_{x3}}{\lambda_3} < \frac{n_{z1}}{\lambda_1} + \frac{n_{x2}}{\lambda_2}; \frac{n_{z1}}{\lambda_1} + \frac{n_{y2}}{\lambda_2} < \frac{n_{y3}}{\lambda_3}$	$\frac{n_{x1}}{\lambda_1} + \frac{n_{z2}}{\lambda_2} > \frac{n_{z3}}{\lambda_3} > \frac{n_{y1}}{\lambda_1} + \frac{n_{z2}}{\lambda_2}$
	*c**	$\frac{n_{z1}}{\lambda_1} + \frac{n_{x2}}{\lambda_2} < \frac{n_{x3}}{\lambda_3}; \frac{n_{y3}}{\lambda_3} < \frac{n_{z1}}{\lambda_1} + \frac{n_{y2}}{\lambda_2}$	$\frac{n_{x1}}{\lambda_1} + \frac{n_{z2}}{\lambda_2} > \frac{n_{z3}}{\lambda_3} > \frac{n_{y1}}{\lambda_1} + \frac{n_{z2}}{\lambda_2}$
	d	$\frac{n_{y1}}{\lambda_1} + \frac{n_{x2}}{\lambda_2} < \frac{n_{x3}}{\lambda_3} < \frac{n_{z1}}{\lambda_1} + \frac{n_{x2}}{\lambda_2}$	$\frac{n_{y3}}{\lambda_3} > \frac{n_{x1}}{\lambda_1} + \frac{n_{y2}}{\lambda_2}; \frac{n_{x1}}{\lambda_1} + \frac{n_{z2}}{\lambda_2} > \frac{n_{z3}}{\lambda_3}$
	*d**	$\frac{n_{y1}}{\lambda_1} + \frac{n_{x2}}{\lambda_2} < \frac{n_{x3}}{\lambda_3} < \frac{n_{z1}}{\lambda_1} + \frac{n_{x2}}{\lambda_2}$	$\frac{n_{x1}}{\lambda_1} + \frac{n_{y2}}{\lambda_2} > \frac{n_{y3}}{\lambda_3}; \frac{n_{z3}}{\lambda_3} > \frac{n_{x1}}{\lambda_1} + \frac{n_{z2}}{\lambda_2}$
Conditions *c*, *d* are applied if		$\frac{n_{y1}}{\lambda_1} - \frac{n_{x1}}{\lambda_1}, \frac{n_{y2}}{\lambda_2} - \frac{n_{x2}}{\lambda_2} < \frac{n_{y3}}{\lambda_3} - \frac{n_{x3}}{\lambda_3}$	$\frac{n_{y1}}{\lambda_1} - \frac{n_{z1}}{\lambda_1}, \frac{n_{y2}}{\lambda_2} - \frac{n_{z2}}{\lambda_2} < \frac{n_{y3}}{\lambda_3} - \frac{n_{z3}}{\lambda_3}$
Conditions *c**, *d** are applied if		$\frac{n_{y3}}{\lambda_3} - \frac{n_{x3}}{\lambda_3} < \frac{n_{y1}}{\lambda_1} - \frac{n_{x1}}{\lambda_1}, \frac{n_{y2}}{\lambda_2} - \frac{n_{x2}}{\lambda_2}$	$\frac{n_{y3}}{\lambda_3} - \frac{n_{z3}}{\lambda_3} < \frac{n_{y1}}{\lambda_1} - \frac{n_{z1}}{\lambda_1}, \frac{n_{y2}}{\lambda_2} - \frac{n_{z2}}{\lambda_2}$

Tables 1.7.3.5 and 1.7.3.6 give, respectively, the inequalities that determine collinear phase matching in the principal planes for the three types of three-wave SFG and for the seven types of four-wave SFG.

The inequalities in Table 1.7.3.5 show that a phase-matching cone which would join the directions *a* and *d* is not possible for any type of interaction, because the corresponding inequalities have an opposite sense. It is the same for a hypothetical cone joining *b* and *c*.

The existence of type-II or type-III SFG phase matching imposes the existence of type I, because the inequalities relative to type I are always satisfied whenever type II or type III exists. However, type I can exist even if type II or type III is not allowed. A type-I phase-matched SFG in area *c* forbids phase-matching directions in area *b* for type-II and type-III SFG. The exclusion is the same between *d* and *a*. The consideration of all the possible combinations of the inequalities of Table 1.7.3.5 leads to 84 possible classes of phase-matching cones for both positive and negative biaxial crystals (Fève *et al.*, 1993; Fève, 1994). There are 14 classes for second harmonic generation (SHG) which correspond to the degenerated case ($\omega_1 = \omega_2$) (Hobden, 1967).

The coexistence of the different types of four-wave phase matching is limited as for the three-wave case: a cone joining *a* and *d* or *b* and *c* is impossible for type-I SFG. Type I in area *d*

Table 1.7.3.6. *Refractive-index conditions that determine collinear phase-matching loci in the principal planes of positive and negative biaxial crystals for four-wave SFG*

The types corresponding to the different DFGs are given in Table 1.7.3.2 (Boulanger *et al.*, 1993).

(*a*) SFG type I.

Phase-matching loci in the principal planes	Inequalities determining four-wave collinear phase matching in biaxial crystals	
	Positive sign	Negative sign
a	$\frac{n_{x4}}{\lambda_4} < \frac{n_{y1}}{\lambda_1} + \frac{n_{y2}}{\lambda_2} + \frac{n_{y3}}{\lambda_3} < \frac{n_{z4}}{\lambda_4}$	$\frac{n_{z1}}{\lambda_1} + \frac{n_{z2}}{\lambda_2} + \frac{n_{z3}}{\lambda_3} < \frac{n_{y4}}{\lambda_4} < \frac{n_{x1}}{\lambda_1} + \frac{n_{x2}}{\lambda_2} + \frac{n_{x3}}{\lambda_3}$
b	$\frac{n_{x1}}{\lambda_1} + \frac{n_{x2}}{\lambda_2} + \frac{n_{x3}}{\lambda_3} < \frac{n_{y4}}{\lambda_4} < \frac{n_{z1}}{\lambda_1} + \frac{n_{z2}}{\lambda_2} + \frac{n_{z3}}{\lambda_3}$	$\frac{n_{z4}}{\lambda_4} < \frac{n_{y1}}{\lambda_1} + \frac{n_{y2}}{\lambda_2} + \frac{n_{y3}}{\lambda_3} < \frac{n_{x4}}{\lambda_4}$
c	$\frac{n_{x4}}{\lambda_4} < \frac{n_{z1}}{\lambda_1} + \frac{n_{z2}}{\lambda_2} + \frac{n_{z3}}{\lambda_3} < \frac{n_{y4}}{\lambda_4}$	$\frac{n_{y1}}{\lambda_1} + \frac{n_{y2}}{\lambda_2} + \frac{n_{y3}}{\lambda_3} < \frac{n_{z4}}{\lambda_4} < \frac{n_{x1}}{\lambda_1} + \frac{n_{x2}}{\lambda_2} + \frac{n_{x3}}{\lambda_3}$
d	$\frac{n_{y1}}{\lambda_1} + \frac{n_{y2}}{\lambda_2} + \frac{n_{y3}}{\lambda_3} < \frac{n_{x4}}{\lambda_4} < \frac{n_{z1}}{\lambda_1} + \frac{n_{z2}}{\lambda_2} + \frac{n_{z3}}{\lambda_3}$	$\frac{n_{z4}}{\lambda_4} < \frac{n_{x1}}{\lambda_1} + \frac{n_{x2}}{\lambda_2} + \frac{n_{x3}}{\lambda_3} < \frac{n_{y4}}{\lambda_4}$

(*b*) SFG type II ($i = 1, j = 2, k = 3$), SFG type III ($i = 3, j = 1, k = 2$), SFG type IV ($i = 2, j = 3, k = 1$).

Phase-matching loci in the principal planes	Inequalities determining four-wave collinear phase matching in biaxial crystals	
	Positive sign	Negative sign
a	$\frac{n_{x4}}{\lambda_4} < \frac{n_{xi}}{\lambda_i} + \frac{n_{xj}}{\lambda_j} + \frac{n_{yk}}{\lambda_k}; \frac{n_{zi}}{\lambda_i} + \frac{n_{zj}}{\lambda_j} + \frac{n_{yk}}{\lambda_k} < \frac{n_{z4}}{\lambda_4}$	$\frac{n_{yi}}{\lambda_i} + \frac{n_{yj}}{\lambda_j} + \frac{n_{zk}}{\lambda_k} < \frac{n_{y4}}{\lambda_4} < \frac{n_{yi}}{\lambda_i} + \frac{n_{yj}}{\lambda_j} + \frac{n_{xk}}{\lambda_k}$
b	$\frac{n_{yi}}{\lambda_i} + \frac{n_{yj}}{\lambda_j} + \frac{n_{xk}}{\lambda_k} < \frac{n_{y4}}{\lambda_4} < \frac{n_{yi}}{\lambda_i} + \frac{n_{yj}}{\lambda_j} + \frac{n_{zk}}{\lambda_k}$	$\frac{n_{z4}}{\lambda_4} < \frac{n_{zi}}{\lambda_i} + \frac{n_{zj}}{\lambda_j} + \frac{n_{yk}}{\lambda_k}; \frac{n_{xi}}{\lambda_i} + \frac{n_{xj}}{\lambda_j} + \frac{n_{yk}}{\lambda_k} < \frac{n_{x4}}{\lambda_4}$
c	$\frac{n_{x4}}{\lambda_4} < \frac{n_{xi}}{\lambda_i} + \frac{n_{xj}}{\lambda_j} + \frac{n_{zk}}{\lambda_k}; \frac{n_{yi}}{\lambda_i} + \frac{n_{yj}}{\lambda_j} + \frac{n_{zk}}{\lambda_k} < \frac{n_{y4}}{\lambda_4}$	$\frac{n_{zi}}{\lambda_i} + \frac{n_{zj}}{\lambda_j} + \frac{n_{yk}}{\lambda_k} < \frac{n_{z4}}{\lambda_4} < \frac{n_{zi}}{\lambda_i} + \frac{n_{zj}}{\lambda_j} + \frac{n_{xk}}{\lambda_k}$
*c**	$\frac{n_{xi}}{\lambda_i} + \frac{n_{xj}}{\lambda_j} + \frac{n_{zk}}{\lambda_k} < \frac{n_{x4}}{\lambda_4}; \frac{n_{y4}}{\lambda_4} < \frac{n_{yi}}{\lambda_i} + \frac{n_{yj}}{\lambda_j} + \frac{n_{zk}}{\lambda_k}$	$\frac{n_{zi}}{\lambda_i} + \frac{n_{zj}}{\lambda_j} + \frac{n_{yk}}{\lambda_k} < \frac{n_{z4}}{\lambda_4} < \frac{n_{zi}}{\lambda_i} + \frac{n_{zj}}{\lambda_j} + \frac{n_{xk}}{\lambda_k}$
d	$\frac{n_{xi}}{\lambda_i} + \frac{n_{xj}}{\lambda_j} + \frac{n_{yk}}{\lambda_k} < \frac{n_{x4}}{\lambda_4} < \frac{n_{xi}}{\lambda_i} + \frac{n_{xj}}{\lambda_j} + \frac{n_{zk}}{\lambda_k}$	$\frac{n_{z4}}{\lambda_4} < \frac{n_{zi}}{\lambda_i} + \frac{n_{zj}}{\lambda_j} + \frac{n_{xk}}{\lambda_k}; \frac{n_{yi}}{\lambda_i} + \frac{n_{yj}}{\lambda_j} + \frac{n_{xk}}{\lambda_k} < \frac{n_{y4}}{\lambda_4}$
*d**	$\frac{n_{xi}}{\lambda_i} + \frac{n_{xj}}{\lambda_j} + \frac{n_{yk}}{\lambda_k} < \frac{n_{x4}}{\lambda_4} < \frac{n_{xi}}{\lambda_i} + \frac{n_{xj}}{\lambda_j} + \frac{n_{zk}}{\lambda_k}$	$\frac{n_{zi}}{\lambda_i} + \frac{n_{zj}}{\lambda_j} + \frac{n_{xk}}{\lambda_k} < \frac{n_{z4}}{\lambda_4}; \frac{n_{y4}}{\lambda_4} < \frac{n_{yi}}{\lambda_i} + \frac{n_{yj}}{\lambda_j} + \frac{n_{xk}}{\lambda_k}$
SFG type II $(i, j) = (1, 2)$; SFG type III $(i, j) = (1, 3)$; SFG type IV $(i, j) = (2, 3)$		
Conditions *c*, *d* are applied if	$\frac{n_{yi}}{\lambda_i} + \frac{n_{yj}}{\lambda_j} - \frac{n_{xi}}{\lambda_i} - \frac{n_{xj}}{\lambda_j} < \frac{n_{y4}}{\lambda_4} - \frac{n_{x4}}{\lambda_4}$	$\frac{n_{yi}}{\lambda_i} + \frac{n_{yj}}{\lambda_j} - \frac{n_{zi}}{\lambda_i} - \frac{n_{zj}}{\lambda_j} < \frac{n_{y4}}{\lambda_4} - \frac{n_{z4}}{\lambda_4}$
Conditions *c**, *d** are applied if	$\frac{n_{y4}}{\lambda_4} - \frac{n_{x4}}{\lambda_4} < \frac{n_{yi}}{\lambda_i} + \frac{n_{yj}}{\lambda_j} - \frac{n_{xi}}{\lambda_i} - \frac{n_{xj}}{\lambda_j}$	$\frac{n_{y4}}{\lambda_4} - \frac{n_{z4}}{\lambda_4} < \frac{n_{yi}}{\lambda_i} + \frac{n_{yj}}{\lambda_j} - \frac{n_{zi}}{\lambda_i} - \frac{n_{zj}}{\lambda_j}$

forbids the six other types in *a*. The same restriction exists between *c* and *b*. Types II, III, IV, V[4], VI[4] and VII[4] cannot exist without type I; other restrictions concern the relations between types II, III, IV and types V[4], VI[4], VII[4] (Fève, 1994). The counting of the classes of four-wave phase-matching cones obtained from all the possible combinations of the inequalities of Table 1.7.3.6 is complex and it has not yet been done.

For reasons explained later, it can be interesting to consider a non-collinear interaction. In this case, the projection of the vectorial phase-matching relation (1.7.3.26) on the wavevector $\mathbf{k}(\omega_\gamma, \theta_\gamma, \varphi_\gamma)$ of highest frequency ω_γ leads to

$$\sum_{i=1}^{\gamma-1} \omega_i n(\omega_i, \theta_i, \varphi_i) \cos \alpha_{i\gamma} = \omega_\gamma n(\omega_\gamma, \theta_\gamma, \varphi_\gamma), \qquad (1.7.3.29)$$

where $\alpha_{i\gamma}$ is the angle between $\mathbf{k}(\omega_i, \theta_i, \varphi_i)$ and $\mathbf{k}(\omega_\gamma, \theta_\gamma, \varphi_\gamma)$, with $\gamma = 3$ for a three-wave interaction and $\gamma = 4$ for a four-wave interaction. The phase-matching angles $(\theta_\gamma, \varphi_\gamma)$ can be expressed as a function of the different (θ_i, φ_i) by the projection of (1.7.3.26) on the three principal axes of the optical frame.

The configurations of polarization allowing non-collinear phase matching are the same as for collinear phase matching. Furthermore, non-collinear phase matching exists only if collinear phase matching is allowed; the converse is not true (Fève, 1994). Note that collinear or non-collinear phase-matching conditions are rarely satisfied over the entire transparency range of the crystal.

1.7.3.2.3. *Quasi phase matching*

When index matching is not allowed, it is possible to increase the energy of the generated wave continuously during the propagation by introducing a periodic change in the sign of the nonlinear electric susceptibility, which leads to a periodic reset of

Table 1.7.3.6 (*cont.*)

(*c*) SFG type V^4 ($i = 1, j = 2, k = 3$), SFG type VI^4 ($i = 2, j = 3, k = 1$), SFG type VII^4 ($i = 3, j = 1, k = 2$).

Phase-matching loci in the principal planes	Inequalities determining four-wave collinear phase matching in biaxial crystals	
	Positive sign	Negative sign
a	$\frac{n_{x4}}{\lambda_4} < \frac{n_{xi}}{\lambda_i} + \frac{n_{yj}}{\lambda_j} + \frac{n_{yk}}{\lambda_k}; \frac{n_{zi}}{\lambda_i} + \frac{n_{yj}}{\lambda_j} + \frac{n_{yk}}{\lambda_k} < \frac{n_{z4}}{\lambda_4}$	$\frac{n_{yi}}{\lambda_i} + \frac{n_{zj}}{\lambda_j} + \frac{n_{zk}}{\lambda_k} < \frac{n_{y4}}{\lambda_4} < \frac{n_{yi}}{\lambda_i} + \frac{n_{xj}}{\lambda_j} + \frac{n_{xk}}{\lambda_k}$
b	$\frac{n_{yi}}{\lambda_i} + \frac{n_{xj}}{\lambda_j} + \frac{n_{xk}}{\lambda_k} < \frac{n_{y4}}{\lambda_4} < \frac{n_{yi}}{\lambda_i} + \frac{n_{zj}}{\lambda_j} + \frac{n_{zk}}{\lambda_k}$	$\frac{n_{z4}}{\lambda_4} < \frac{n_{zi}}{\lambda_i} + \frac{n_{yj}}{\lambda_j} + \frac{n_{yk}}{\lambda_k}; \frac{n_{xi}}{\lambda_i} + \frac{n_{yj}}{\lambda_j} + \frac{n_{yk}}{\lambda_k} < \frac{n_{x4}}{\lambda_4}$
c′	$\frac{n_{x4}}{\lambda_4} < \frac{n_{xi}}{\lambda_i} + \frac{n_{zj}}{\lambda_j} + \frac{n_{zk}}{\lambda_k}; \frac{n_{yi}}{\lambda_i} + \frac{n_{zj}}{\lambda_j} + \frac{n_{zk}}{\lambda_k} < \frac{n_{y4}}{\lambda_4}$	$\frac{n_{zi}}{\lambda_i} + \frac{n_{yj}}{\lambda_j} + \frac{n_{yk}}{\lambda_k} < \frac{n_{z4}}{\lambda_4} < \frac{n_{zi}}{\lambda_i} + \frac{n_{xj}}{\lambda_j} + \frac{n_{xk}}{\lambda_k}$
*c***	$\frac{n_{xi}}{\lambda_i} + \frac{n_{zj}}{\lambda_j} + \frac{n_{zk}}{\lambda_k} < \frac{n_{x4}}{\lambda_4}; \frac{n_{y4}}{\lambda_4} < \frac{n_{yi}}{\lambda_i} + \frac{n_{zj}}{\lambda_j} + \frac{n_{zk}}{\lambda_k}$	$\frac{n_{zi}}{\lambda_i} + \frac{n_{yj}}{\lambda_j} + \frac{n_{yk}}{\lambda_k} < \frac{n_{z4}}{\lambda_4} < \frac{n_{zi}}{\lambda_i} + \frac{n_{xj}}{\lambda_j} + \frac{n_{xk}}{\lambda_k}$
d′	$\frac{n_{xi}}{\lambda_i} + \frac{n_{yj}}{\lambda_j} + \frac{n_{yk}}{\lambda_k} < \frac{n_{x4}}{\lambda_4} < \frac{n_{xi}}{\lambda_i} + \frac{n_{zj}}{\lambda_j} + \frac{n_{zk}}{\lambda_k}$	$\frac{n_{z4}}{\lambda_4} < \frac{n_{zi}}{\lambda_i} + \frac{n_{xj}}{\lambda_j} + \frac{n_{xk}}{\lambda_k}; \frac{n_{yi}}{\lambda_i} + \frac{n_{xj}}{\lambda_j} + \frac{n_{xk}}{\lambda_k} < \frac{n_{y4}}{\lambda_4}$
*d***	$\frac{n_{xi}}{\lambda_i} + \frac{n_{yj}}{\lambda_j} + \frac{n_{yk}}{\lambda_k} < \frac{n_{x4}}{\lambda_4} < \frac{n_{xi}}{\lambda_i} + \frac{n_{zj}}{\lambda_j} + \frac{n_{zk}}{\lambda_k}$	$\frac{n_{zi}}{\lambda_i} + \frac{n_{xj}}{\lambda_j} + \frac{n_{xk}}{\lambda_k} < \frac{n_{z4}}{\lambda_4}; \frac{n_{y4}}{\lambda_4} < \frac{n_{yi}}{\lambda_i} + \frac{n_{xj}}{\lambda_j} + \frac{n_{xk}}{\lambda_k}$
SFG type V^4, ($i = 1$); SFG type VI^4 ($i = 2$) ; SFG type VII^4 ($i = 3$)		
Conditions *c*′, *d*′ are applied if	$\frac{n_{yi}}{\lambda_i} - \frac{n_{xi}}{\lambda_i} < \frac{n_{y4}}{\lambda_4} - \frac{n_{x4}}{\lambda_4}$	$\frac{n_{yi}}{\lambda_i} - \frac{n_{zi}}{\lambda_i} < \frac{n_{y4}}{\lambda_4} - \frac{n_{z4}}{\lambda_4}$
Conditions *c***, *d*** are applied if	$\frac{n_{y4}}{\lambda_4} - \frac{n_{x4}}{\lambda_4} < \frac{n_{yi}}{\lambda_i} - \frac{n_{xi}}{\lambda_i}$	$\frac{n_{y4}}{\lambda_4} - \frac{n_{z4}}{\lambda_4} < \frac{n_{yi}}{\lambda_i} - \frac{n_{zi}}{\lambda_i}$

π between the waves (Armstrong *et al.*, 1962). This method is called quasi phase matching (QPM). The transfer of energy between the nonlinear polarization and the generated electric field never alternates if the reset is made at each coherence length. In this case and for a three-wave SFG, the nonlinear polarization sequence is the following:

(i) from 0 to L_c, $\mathbf{P}^{NL}(\omega_3) = \varepsilon_0\chi^{(2)}(\omega_3)\mathbf{e}_1\mathbf{e}_2E_1E_2\exp\{i[k(\omega_1) + k(\omega_2)]Z\}$;

(ii) from L_c to $2L_c$, $\mathbf{P}^{NL}(\omega_3) = -\varepsilon_0\chi^{(2)}(\omega_3)\mathbf{e}_1\mathbf{e}_2E_1E_2\exp\{i[k(\omega_1) + k(\omega_2)]Z\}$, which is equivalent to $\mathbf{P}^{NL}(\omega_3) = \varepsilon_0\chi^{(2)}(\omega_3)\mathbf{e}_1\mathbf{e}_2E_1E_2\exp(i\{[k(\omega_1) + k(\omega_2)]Z - \pi\})$.

QPM devices are a recent development and are increasingly being considered for applications (Fejer *et al.*, 1992). The nonlinear medium can be formed by the bonding of thin wafers alternately rotated by π; this has been done for GaAs (Gordon *et al.*, 1993). For ferroelectric crystals, it is possible to form periodic reversing of the spontaneous polarization in the same sample by proton- or ion-exchange techniques, or by applying an electric field, which leads to periodically poled (pp) materials like ppLiNbO$_3$ or ppKTiOPO$_4$ (Myers *et al.*, 1995; Karlsson & Laurell, 1997; Rosenman *et al.*, 1998).

Quasi phase matching offers three main advantages when compared with phase matching: it may be used for any configuration of polarization of the interacting waves, which allows us to use the largest coefficient of the $\chi^{(2)}$ tensor, as explained in the following section; QPM can be achieved over the entire transparency range of the crystal, since the periodicity can be adjusted; and, finally, double refraction and its harmful effect on the nonlinear efficiency can be avoided because QPM can be realized in the principal plane of a uniaxial crystal or in the principal axes of biaxial crystals. Nevertheless, there are limitations due to the difficulty in fabricating the corresponding materials: diffusion-bonded GaAs has strong reflection losses and periodic patterns of ppKTP or ppLN can only be written over a thickness that does not exceed 3 mm, which limits the input energy.

1.7.3.2.4. *Effective coefficient and field tensor*

1.7.3.2.4.1. *Definitions and symmetry properties*

The refractive indices and their dispersion in frequency determine the existence and loci of the phase-matching directions, and so impose the direction of the unit electric field vectors of the interacting waves according to (1.7.3.9). The effective coefficient, given by (1.7.3.23) and (1.7.3.25), depends in part on the linear optical properties *via* the field tensor, which is the tensor product of the interacting unit electric field vectors (Boulanger, 1989; Boulanger & Marnier, 1991; Boulanger *et al.*, 1993; Zyss, 1993). Indeed, the effective coefficient is the contraction between the field tensor and the electric susceptibility tensor of corresponding order:

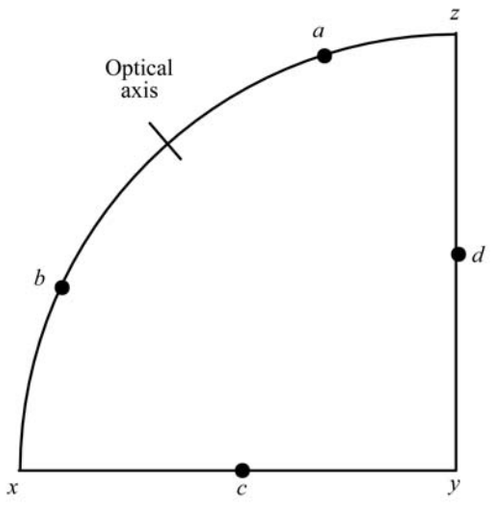

Fig. 1.7.3.5. Stereographic projection on the optical frame of the possible loci of phase-matching directions in the principal planes of a biaxial crystal.

(i) For three-wave mixing,

$$\chi^{(2)}_{\rm eff}(\omega_a, \omega_b, \omega_c, \theta, \varphi) = \sum_{ijk} \chi_{ijk}(\omega_a) F_{ijk}(\omega_a, \omega_b, \omega_c, \theta, \varphi) = \chi^{(2)}(\omega_a) \cdot F^{(2)}(\omega_a, \omega_b, \omega_c, \theta, \varphi), \quad (1.7.3.30)$$

with

$$F^{(2)}(\omega_a, \omega_b, \omega_c, \theta, \varphi) = \mathbf{e}(\omega_a, \theta, \varphi) \otimes \mathbf{e}(\omega_b, \theta, \varphi) \otimes \mathbf{e}(\omega_c, \theta, \varphi), \quad (1.7.3.31)$$

where $\omega_a, \omega_b, \omega_c$ correspond to $\omega_3, \omega_1, \omega_2$ for SFG ($\omega_3 = \omega_1 + \omega_2$); to $\omega_1, \omega_3, \omega_2$ for DFG ($\omega_1 = \omega_3 - \omega_2$); and to $\omega_2, \omega_3, \omega_1$ for DFG ($\omega_2 = \omega_3 - \omega_1$).

(ii) For four-wave mixing,

$$\chi^{(3)}_{\rm eff}(\omega_a, \omega_b, \omega_c, \omega_d, \theta, \varphi) = \sum_{ijkl} \chi_{ijkl}(\omega_a) F_{ijkl}(\omega_a, \omega_b, \omega_c, \omega_d, \theta, \varphi) = \chi^{(3)}(\omega_a) \cdot F^{(3)}(\omega_a, \omega_b, \omega_c, \omega_d, \theta, \varphi), \quad (1.7.3.32)$$

with

$$F^{(3)}(\omega_a, \omega_b, \omega_c, \omega_d \theta, \varphi) = \mathbf{e}(\omega_a, \theta, \varphi) \otimes \mathbf{e}(\omega_b, \theta, \varphi) \otimes \mathbf{e}(\omega_c, \theta, \varphi) \otimes \mathbf{e}(\omega_d, \theta, \varphi), \quad (1.7.3.33)$$

where $\omega_a, \omega_b, \omega_c, \omega_d$ correspond to $\omega_4, \omega_1, \omega_2, \omega_3$ for SFG ($\omega_4 = \omega_1 + \omega_2 + \omega_3$); to $\omega_1, \omega_4, \omega_2, \omega_3$ for DFG ($\omega_1 = \omega_4 - \omega_2 - \omega_3$); to $\omega_2, \omega_4, \omega_1, \omega_3$ for DFG ($\omega_2 = \omega_4 - \omega_1 - \omega_3$); and to ω_3, ω_4, ω_1, ω_2 for DFG ($\omega_3 = \omega_4 - \omega_1 - \omega_2$).

Each $\mathbf{e}(\omega_i, \theta, \varphi)$ corresponds to a given eigen electric field vector.

The components of the field tensor are trigonometric functions of the direction of propagation.

Particular relations exist between field-tensor components of SFG and DFG which are valid for any direction of propagation. Indeed, from (1.7.3.31) and (1.7.3.33), it is obvious that the field-tensor components remain unchanged by concomitant permutations of the electric field vectors at the different frequencies and the corresponding Cartesian indices (Boulanger & Marnier, 1991; Boulanger *et al.*, 1993):

$$F^{\mathbf{e}_3\mathbf{e}_1\mathbf{e}_2}_{ijk}(\omega_3 = \omega_1 + \omega_2) = F^{\mathbf{e}_1\mathbf{e}_3\mathbf{e}_2}_{jik}(\omega_1 = \omega_3 - \omega_2) = F^{\mathbf{e}_2\mathbf{e}_3\mathbf{e}_1}_{kij}(\omega_2 = \omega_3 - \omega_1) \quad (1.7.3.34)$$

and

$$\begin{aligned} &F^{\mathbf{e}_4\mathbf{e}_1\mathbf{e}_2\mathbf{e}_3}_{ijkl}(\omega_4 = \omega_1 + \omega_2 + \omega_3) \\ &= F^{\mathbf{e}_1\mathbf{e}_4\mathbf{e}_2\mathbf{e}_3}_{jikl}(\omega_1 = \omega_4 - \omega_2 - \omega_3) \\ &= F^{\mathbf{e}_2\mathbf{e}_4\mathbf{e}_1\mathbf{e}_3}_{kijl}(\omega_2 = \omega_4 - \omega_1 - \omega_3) \\ &= F^{\mathbf{e}_3\mathbf{e}_4\mathbf{e}_1\mathbf{e}_2}_{lijk}(\omega_3 = \omega_4 - \omega_1 - \omega_2), \end{aligned} \quad (1.7.3.35)$$

where $\mathbf{e}_i$ is the unit electric field vector at ω_i.

For a given interaction, the symmetry of the field tensor is governed by the vectorial properties of the electric fields, detailed in Section 1.7.3.1. This symmetry is then characteristic of both the optical class and the direction of propagation. These properties lead to four kinds of relations between the field-tensor components described later (Boulanger & Marnier, 1991; Boulanger *et al.*, 1993). Because of their interest for phase matching, we consider only the uniaxial and biaxial classes.

(*a*) The number of zero components varies with the direction of propagation according to the existence of nil electric field vector components. The only case where all the components are nonzero concerns any direction of propagation out of the principal planes in biaxial crystals.

(*b*) The orthogonality relation (1.7.3.10) between any ordinary and extraordinary waves propagating in the same direction leads to specific relations independent of the direction of propagation. For example, the field tensor of an (*eooo*) configuration of polarization (one extraordinary wave relative to the first Cartesian index and three ordinary waves relative to the three other indices) verifies $F_{xxij} + F_{yyij}$ $(+ F_{zzij} = 0) =$ $F_{xixj} + F_{yiyj}$ $(+ F_{zizj} = 0) = F_{xijx} + F_{yijy}$ $(+ F_{zijz} = 0) = 0$, with i and j equal to x or y; the combination of these three relations leads to $F_{xxxx} = -F_{yyxx} = -F_{yxyx} = -F_{yxxy}$, $F_{yyyy} = -F_{xxyy} = -F_{xyxy} = -F_{xyyx}$ and $F_{yxyy} = F_{yyxy} = F_{yyyx} = -F_{xyxx} = F_{xxyx} = -F_{xxxy}$. In a biaxial crystal, this kind of relation does not exist out of the principal planes.

(*c*) The fact that the direction of the ordinary electric field vectors in uniaxial crystals does not depend on the frequency, (1.7.3.11), leads to symmetry in the Cartesian indices relative to the ordinary waves. These relations can be redundant in comparison with certain orthogonality relations and are valid for any direction of propagation in uniaxial crystals. It is also the case for biaxial crystals, but only in the principal planes xz and yz. In the xy plane of biaxial crystals, the ordinary wave, (1.7.3.15), has a walk-off angle which depends on the frequency, and the extraordinary wave, (1.7.3.16), has no walk-off angle: then the field tensor is symmetric in the Cartesian indices relative to the extraordinary waves. The walk-off angles of ordinary and extraordinary waves are nil along the principal axes of the index surface of biaxial and uniaxial crystals and so everywhere in the xy plane of uniaxial crystals. Thus, any field tensor associated with these directions of propagation is symmetric in the Cartesian indices relative to both the ordinary and extraordinary waves.

(*d*) Equalities between frequencies can create new symmetries: the field tensors of the uniaxial class for any direction of propagation and of the biaxial class in only the principal planes xz and yz become symmetric in the Cartesian indices relative to the extraordinary waves at the same frequency; in the xy plane of a biaxial crystal, this symmetry concerns the indices relative to the ordinary waves. Equalities between frequencies are the only situations for which the field tensors are partly symmetric out of the principal planes of a biaxial crystal: the symmetry concerns the indices relative to the waves (+) with identical frequencies; it is the same for the waves (−): for example, $F^{-++}_{ijk}(2\omega = \omega + \omega) = F^{-++}_{ikj}(2\omega = \omega + \omega)$, $F^{-++-}_{ijkl}(\omega_4 = \omega + \omega + \omega_3) = F^{-++-}_{ikjl}(\omega_4 = \omega + \omega + \omega_3)$, $F^{-++-}_{ijkl}(\omega_4 = \omega + \omega + \omega_3) = F^{--+-}_{ikjl}(\omega_4 = \omega + \omega + \omega_3)$ and so on.

1.7.3.2.4.2. *Uniaxial class*

The field-tensor components are calculated from (1.7.3.11) and (1.7.3.12). The phase-matching case is the only one considered here: according to Tables 1.7.3.1 and 1.7.3.2, the allowed configurations of polarization of three-wave and four-wave interactions, respectively, are the 2*o.e* (two ordinary and one extraordinary waves), the 2*e.o* and the 3*o.e*, 3*e.o*, 2*o.*2*e*.

Tables 1.7.3.7 and 1.7.3.8 give, respectively, the matrix representations of the three-wave interactions (*eoo*), (*oee*) and of the four-wave (*oeee*), (*eooo*), (*ooee*) interactions for any direction of propagation in the general case where all the frequencies are different. In this situation, the number of independent components of the field tensors are: 7 for 2*o.e*, 12 for 2*e.o*, 9 for 3*o.e*, 28 for 3*e.o* and 16 for 2*o.*2*e*. Note that the increase of the number of ordinary waves leads to an enhancement of symmetry of the field tensors.

If there are equalities between frequencies, the field tensors *oee*, *oeee* and *ooee* become totally symmetric in the Cartesian indices relative to the extraordinary waves and the tensors *eoo* and *eooo* remain unchanged.

Table 1.7.3.9 gives the field-tensor components specifically nil in the principal planes of uniaxial and biaxial crystals. The nil

components for the other configurations of polarization are obtained by permutation of the Cartesian indices and the corresponding polarizations.

From Tables 1.7.3.7 and 1.7.3.8, it is possible to deduce all the other 2*e.o* interactions (*eeo*), (*eoe*), the 2*o.e* interactions (*ooe*), (*oeo*), the 3*o.e* interactions (*oooe*), (*oeoo*), (*ooeo*), the 3*e.o* interactions (*eoee*), (*eeoe*), (*eeeo*) and the 2*o*.2*e* interactions (*oeoe*), (*eoeo*), (*eeoo*), (*oeeo*), (*eooe*). The corresponding interactions and types are given in Tables 1.7.3.1 and 1.7.3.2. According to (1.7.3.31) and (1.7.3.33), the magnitudes of two permutated components are equal if the permutation of polarizations are associated with the corresponding frequencies. For example, according to Table 1.7.3.2, two permutated field-tensor components have the same magnitude for permutation between the following 3*o.e* interactions:

(i) (*eooo*) SFG (ω_4) type I < 0 and the three (*oeoo*) interactions, DFG (ω_1) type II < 0, DFG (ω_2) type III < 0, DFG (ω_3) type IV < 0;

(ii) the three (*oooe*) interactions, SFG (ω_4) type II > 0, DFG (ω_1) type III > 0, DFG (ω_2) type IV > 0 and (*eooo*) DFG (ω_3) type I > 0;

(iii) the two (*ooeo*) interactions SFG (ω_4) type III > 0, DFG (ω_1) type IV > 0, (*eooo*) DFG (ω_2) type I > 0, and (*oooe*) DFG (ω_3) type II > 0;

(iv) (*oeoo*) SFG (ω_4) type IV > 0, (*eooo*) DFG (ω_1) type I > 0, and the two interactions (*ooeo*) DFG (ω_2) type II > 0, DFG (ω_3) type III > 0.

The contraction of the field tensor and the uniaxial dielectric susceptibility tensor of corresponding order, given in Tables 1.7.2.2 to 1.7.2.5, is nil for the following uniaxial crystal classes

Table 1.7.3.7. *Matrix representations of the (oee) and (eoo) field tensors of the uniaxial class and of the biaxial class in the principal planes xz and yz, with* $\omega_1 \neq \omega_2$ *(Boulanger & Marnier, 1991)*

• $F_{ijk} = 0$ ●—● , ○—○ $F_{ijk} = F_{lmn}$ ●—○ $F_{ijk} = -F_{lmn}$

Interactions	Three-rank $F_{ijk}(\theta, \varphi)$ field tensors
Type *eoo* SFG (ω_3) type I < 0 DFG (ω_1) type I > 0 DFG (ω_2) type I > 0	$F =$ (xx yy zz yz zy xz zx xy yx; x, y, z)
Type *oee* SFG (ω_3) type I > 0 DFG (ω_1) type I < 0 DFG (ω_2) type I < 0	$F =$ (xx yy zz yz zy xz zx xy yx; x, y, z)

Table 1.7.3.8. *Matrix representations of the (oeee), (eooo) and (ooee) field tensors of the uniaxial class and of the biaxial class in the principal planes xz and yz, with* $\omega_1 \neq \omega_2 \neq \omega_3$ *(Boulanger et al., 1993)*

• $F_{ijkl} = 0$ ●—● $F_{ijkl} = F_{mnop}$ ●—○ $F_{ijkl} = -F_{mnop}$

Interactions	Four-rank $F_{ijkl}(\theta, \varphi)$ field tensors
Type *oeee* SFG(ω_4) type I > 0 DFG (ω_1) type I < 0 DFG (ω_2) type I < 0 DFG (ω_3) type I < 0	$F(3) =$ (xxx yyy zzz yzz zyz zzy yyz yzy zyy xzz zxz zzx xxz xzx zxx xyy yxy yyx xxy xyx yxx xyz xzy yxz yzx zxy zyx; x, y, z)
Type *eooo* SFG (ω_4) type I < 0 DFG (ω_1) type I > 0 DFG (ω_2) type I > 0 DFG (ω_3) type I > 0	$F(3) =$ (xxx yyy zzz yzz zyz zzy yyz yzy zyy xzz zxz zzx xxz xzx zxx xyy yxy yyx xxy xyx yxx xyz xzy yxz yzx zxy zyx; x, y, z)
Type *ooee* SFG (ω_4) type $V^4 > 0$ DFG (ω_1) type $V^1 > 0$ DFG (ω_2) type $V^2 > 0$ DFG (ω_3) type $V^3 > 0$	$F(3) =$ (xxx yyy zzz yzz zyz zzy yyz yzy zyy xzz zxz zzx xxz xzx zxx xyy yxy yyx xxy xyx yxx xyz xzy yxz yzx zxy zyx; x, y, z)

Table 1.7.3.9. *Field-tensor components specifically nil in the principal planes of uniaxial and biaxial crystals for three-wave and four-wave interactions* $(i, j, k) = x, y$ or z.

Configurations of polarization	Nil field-tensor components		
	(xy) plane	(xz) plane	(yz) plane
eoo	$F_{xjk} = 0$; $F_{yjk} = 0$	$F_{ixk} = F_{ijx} = 0$ $F_{yjk} = 0$	$F_{iyk} = F_{ijy} = 0$ $F_{xjk} = 0$
oee	$F_{ixk} = F_{ijx} = 0$ $F_{iyk} = F_{ijy} = 0$	$F_{iyk} = F_{ijy} = 0$ $F_{xik} = 0$	$F_{ixk} = F_{ijx} = 0$ $F_{yjk} = 0$
eooo	$F_{xjkl} = 0$; $F_{yjkl} = 0$	$F_{ixkl} = F_{ijxl} = F_{ijkx} = 0$ $F_{yjkl} = 0$	$F_{iykl} = F_{ijyl} = F_{ijky} = 0$ $F_{xjkl} = 0$
oeee	$F_{ixkl} = F_{ijxl} = F_{ijkx} = 0$ $F_{iykl} = F_{ijyl} = F_{ijky} = 0$	$F_{iykl} = F_{ijyl} = F_{ijky} = 0$ $F_{xjkl} = 0$	$F_{ixkl} = F_{ijxl} = F_{ijkx} = 0$ $F_{yjkl} = 0$
ooee	$F_{ijxl} = F_{ijkx} = 0$ $F_{ijyl} = F_{ijky} = 0$	$F_{xjkl} = F_{ixkl} = 0$ $F_{ijyl} = F_{ijky} = 0$	$F_{yjkl} = F_{iykl} = 0$ $F_{ijxl} = F_{ijkx} = 0$

and configurations of polarization: D_4 and D_6 for $2o.e$, C_{4v} and C_{6v} for $2e.o$, D_6, D_{6h}, D_{3h} and C_{6v} for $3o.e$ and $3e.o$. Thus, even if phase-matching directions exist, the effective coefficient in these situations is nil, which forbids the interactions considered (Boulanger & Marnier, 1991; Boulanger *et al.*, 1993). The number of forbidden crystal classes is greater under the Kleinman approximation. The forbidden crystal classes have been determined for the particular case of third harmonic generation assuming Kleinman conjecture and without consideration of the field tensor (Midwinter & Warner, 1965).

1.7.3.2.4.3. *Biaxial class*

The symmetry of the biaxial field tensors is the same as for the uniaxial class, though only for a propagation in the principal planes xz and yz; the associated matrix representations are given in Tables 1.7.3.7 and 1.7.3.8, and the nil components are listed in Table 1.7.3.9. Because of the change of optic sign from either side of the optic axis, the field tensors of the interactions for which the phase-matching cone joins areas b and a or a and c, given in Fig. 1.7.3.5, change from one area to another: for example, the field tensor (*eoee*) becomes an (*oeoo*) and so the solicited components of the electric susceptibility tensor are not the same.

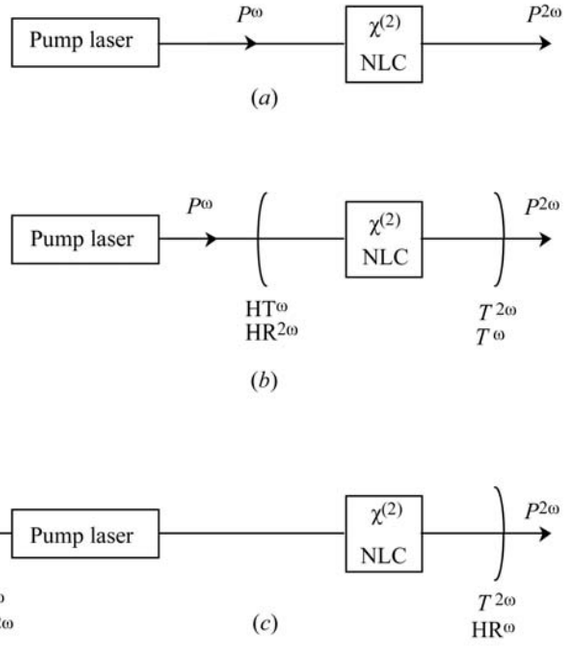

Fig. 1.7.3.6. Schematic configurations for second harmonic generation. (*a*) Non-resonant SHG; (*b*) external resonant SHG: the resonant wave may either be the fundamental or the harmonic one; (*c*) internal resonant SHG. $P^{\omega,2\omega}$ are the fundamental and harmonic powers; HT^{ω} and $HR^{\omega,2\omega}$ are the high-transmission and high-reflection mirrors at ω or 2ω and $T^{\omega,2\omega}$ are the transmission coefficients of the output mirror at ω or 2ω. NLC is the nonlinear crystal with a nonzero $\chi^{(2)}$.

The nonzero field-tensor components for a propagation in the xy plane of a biaxial crystal are: F_{zxx}, F_{zyy}, $F_{zxy} \neq F_{zyx}$ for (*eoo*); F_{xzz}, F_{yzz} for (*oee*); F_{zxxx}, F_{zyyy}, $F_{zxyy} \neq F_{zyxy} \neq F_{zyyx}$, $F_{zxxy} \neq F_{zxyx} \neq F_{zyxx}$ for (*eooo*); F_{xzzz}, F_{yzzz} for (*oeee*); $F_{xyzz} \neq F_{yxzz}$, F_{xxzz}, F_{yyzz} for (*ooee*). The nonzero components for the other configurations of polarization are obtained by the associated permutations of the Cartesian indices and the corresponding polarizations.

The field tensors are not symmetric for a propagation out of the principal planes in the general case where all the frequencies are different: in this case there are 27 independent components for the three-wave interactions and 81 for the four-wave interactions, and so all the electric susceptibility tensor components are solicited.

As phase matching imposes the directions of the electric fields of the interacting waves, it also determines the field tensor and hence the effective coefficient. Thus there is no possibility of choice of the $\chi^{(2)}$ coefficients, since a given type of phase matching is considered. In general, the largest coefficients of polar crystals, *i.e.* χ_{zzz}, are implicated at a very low level when phase matching is achieved, because the corresponding field tensor, *i.e.* F_{zzz}, is often weak (Boulanger *et al.*, 1997). In contrast, QPM authorizes the coupling between three waves polarized along the z axis, which leads to an effective coefficient which is purely χ_{zzz}, *i.e.* $\chi_{\rm eff} = (2/\pi)\chi_{zzz}$, where the numerical factor comes from the periodic character of the rectangular function of modulation (Fejer *et al.*, 1992).

1.7.3.3. *Integration of the propagation equations*

1.7.3.3.1. *Spatial and temporal profiles*

The resolution of the coupled equations (1.7.3.22) or (1.7.3.24) over the crystal length L leads to the electric field amplitude $E_i(X, Y, L)$ of each interacting wave. The general solutions are Jacobian elliptic functions (Armstrong *et al.*, 1962; Fève, Boulanger & Douady, 2002). The integration of the systems is simplified for cases where one or several beams are held constant, which is called the undepleted pump approximation. We consider mainly this kind of situation here. The power of each interacting wave is calculated by integrating the intensity over the cross section of each beam according to (1.7.3.8). For our main purpose, we consider the simple case of plane-wave beams with two kinds of transverse profile:

$$\begin{aligned} &\mathbf{E}(X, Y, Z) = \mathbf{e}E_o(Z) \quad \text{for } (X, Y) \in [-w_o, +w_o] \\ &\mathbf{E}(X, Y, Z) = 0 \qquad\quad \text{elsewhere} \end{aligned} \tag{1.7.3.36}$$

for a flat distribution over a radius w_o;

$$\mathbf{E}(X, Y, Z) = \mathbf{e}E_o(Z)\exp[-(X^2 + Y^2)/w_o^2] \tag{1.7.3.37}$$

for a Gaussian distribution, where w_o is the radius at $(1/e)$ of the electric field and so at $(1/e^2)$ of the intensity.